# The Contribution of Clouds to Northern Hemisphere Surface Temperature Variability on Monthly to Decadal Timescales

Chloe Boehm[1,1] and David W.J. Thompson[2,2]

[1]Colorado State University
[2]University of East Anglia, Colorado State University

January 20, 2023

**Abstract**

Cloud radiative effects (CRE) have well documented impacts on mean climate, and have recently been found to play a key role in climate variability in the tropics. Here we probe the role of CRE in surface temperature variability in the Northern Hemisphere (NH). We compare output from two climate simulations: one in which clouds are coupled to the atmospheric circulation and another in which they are decoupled from the flow. Cloud-circulation coupling leads to widespread increases in NH surface temperature variability, particularly over the oceans and on decadal timescales. Notably, it leads to substantial increases in decadal temperature variability averaged over the North Atlantic and North Pacific basins. The increases derive from the 'reddening' of surface temperature variability by cloud shortwave radiative effects. The results have implications for the interpretation of observed decadal variability, and the importance of cloud-circulation coupling for simulations of decadal variability in climate models.

# The Contribution of Clouds to Northern Hemisphere Surface Temperature Variability on Monthly to Decadal Timescales

**Chloe Boehm[1], David W.J. Thompson[1,2]**

[1]Department of Atmospheric Science, Colorado State University, Fort Collins, CO, USA

[2]School of Environmental Sciences, University of East Anglia, Norwich, UK

Corresponding author: Chloe Boehm (chloe.boehm@colostate.edu)

**Key Points:**

- Coupling between clouds and the atmospheric circulation has a pronounced effect on Northern Hemisphere surface temperature variability
- Coupling leads to notable increases in multiannual to decadal temperature variability in the North Pacific and North Atlantic oceans.
- Increases in surface temperature variability derive primarily from the 'reddening' of variability by cloud shortwave radiative effects.

## Abstract

Cloud radiative effects (CRE) have well documented impacts on mean climate, and have recently been found to play a key role in climate variability in the tropics. Here we probe the role of CRE in surface temperature variability in the Northern Hemisphere (NH). We compare output from two climate simulations: one in which clouds are coupled to the atmospheric circulation and another in which they are decoupled from the flow. Cloud-circulation coupling leads to widespread increases in NH surface temperature variability, particularly over the oceans and on decadal timescales. Notably, it leads to substantial increases in decadal temperature variability averaged over the North Atlantic and North Pacific basins. The increases derive from the 'reddening' of surface temperature variability by cloud shortwave radiative effects. The results have implications for the interpretation of observed decadal variability, and the importance of cloud-circulation coupling for simulations of decadal variability in climate models.

## Plain Language Summary

Clouds play a key role in Earth's climate but their role in climate variability remains unclear, particularly in the extratropics. Here we probe output from climate simulations to demonstrate that coupling between the atmospheric circulation and clouds has a marked influence on surface temperature variability in the Northern Hemisphere. Coupling between clouds and the circulation leads to widespread increases in surface temperature variability, including increases of ~25-45% in the amplitude of multiannual to decadal variability in temperatures averaged over the North Atlantic and North Pacific basins. The results suggest that a notable fraction of the observed decadal variability may derive from cloud processes.


## 1 Introduction

Clouds and their radiative effects play an essential role in governing the mean climate (e.g., Stephens et al., 2012 and references therein). They give rise to some of the most important - and most uncertain - feedbacks under climate change (e.g., Bony & Dufresne, 2005; Zelinka et al., 2010; Bony et al., 2015; Sherwood et al., 2020 and references therein), they play an important role in the dynamical response to climate change (e.g., Albern et al., 2018, 2019, 2020; Ceppi & Hartmann, 2016; Voigt & Albern, 2019; Voigt & Shaw, 2015, 2016; Grise et al., 2019; Voigt et al., 2020 and references therein). And in recent years, it has become clear that they also play an important role in climate variability.

The role of clouds in climate variability has been investigated primarily in the tropics (Rädel et al., 2016; Middlemas et al., 2019; Li et al., 2020). Cloud-radiative effects (CRE) have proven important for simulated variability in the El-Niño/Southern Oscillation (Rädel et al., 2016; Middlemas et al., 2019) and for tropics-wide variations in the sea-surface temperature field (Li et al., 2020). The importance of CRE for extratropical variability is generally less clear, and most studies have focused on the importance of CRE for relatively short-term dynamic variability (Li et al., 2014; Schäfer & Voigt, 2018; Grise et al., 2019; Papavasileiou et al., 2020).

Here we demonstrate that CRE play a fundamental role in simulated surface temperature variability not only in the tropics (e.g., Rädel et al., 2016; Middlemas et al., 2019; Li et al., 2020) but also in the extratropics. Importantly, the coupling between CRE and the atmospheric circulation leads to robust increases in the amplitude of multiannual to decadal variability in surface temperatures averaged over the North Pacific and North Atlantic basins. The results have

potentially important implications for both the interpretation of observed Northern Hemisphere (NH) temperature variability.

## 2 Output and analysis

The role of CRE in extratropical surface temperature variability is quantified by comparing output from two simulations run on a fully-coupled Earth System Model: an "interactive" or control simulation where CREs are coupled to the atmospheric circulation; and a "locked" simulation where CREs are decoupled from the flow. The experiments were conducted by D. Olonscheck at the Max Planck Institute for Meteorology and are identical to those described in detail in Li et al. (2020). In short:

The simulations were run on the Max Planck Institute Earth System Model at T63 (200 km) horizontal resolution and with 47 vertical levels in the atmosphere, and at 1.5 (150 km) horizontal resolution and with 40 vertical levels in the ocean. The interactive simulation was run for 250 years with preindustrial forcing but we use only the last 200 years of the simulation to account for model spin-up. The locked simulation was performed in the same way, except that all cloud parameters were randomized before being read into the radiation code. This was accomplished by 1) saving cloud parameters at every two hour radiation call from the interactive simulation; 2) randomizing the order of the years but not the hours or days associated with the cloud properties at each time step; and 3) reading the randomized cloud fields into the radiation code at every two hour time step when running the locked simulation. As such, the cloud parameters in the locked simulation have the same long-term mean diurnal and seasonal cycles as those in the interactive simulation, but they are decoupled from variability in the atmospheric circulation on all timescales. For details on the locking methodology see Rädel et al. (2016), Olonscheck et al. (2019), and Li et al. (2020); for details on the experiments used here see Li et al. (2020).

The amplitude of surface temperature variability is found as the standard deviation. The changes in variability between the locked simulations is given as $\frac{\boldsymbol{s_i}}{\boldsymbol{s_l}} - \mathbf{1}$, where $\boldsymbol{s_i}$ and $\boldsymbol{s_l}$ denote the standard deviations from the interactive and locked runs, respectively. Time filtering is done using a Butterworth filter.

As noted above, the output is the same as that used in our recent study (Li et al., 2020). In that work, we focused on the tropics and did not identify large changes in surface temperature variability in the extratropics. In part, that is because we did not explore results for the Northern Hemisphere in depth, and we did not consider temperature variability on annual to decadal timescales. Here we focus on the Northern Hemisphere.

## 3 The Contribution of Clouds to Northern Hemisphere Surface Temperature Variability

Figures 1-4 compare surface temperature variability in the interactive and locked simulations. The climatological standard deviations from the interactive and locked runs are shown in the left and middle columns of Fig. 1, respectively. Results for the ocean areas are shown in the top row; results for land areas are shown in the bottom row. Note that the colorscale

is different in the two rows. In both simulations, the largest standard deviations are found over the Arctic, the NH land areas, and the Gulf Stream and Kuroshio Current regions. The fractional changes in the standard deviations ( $\frac{s_i}{s_l} - 1$) are shown in the right column. To first order, coupling between CRE and the atmospheric circulation leads to widespread increases in surface temperature variability over the North Pacific, North America, and Eurasia (panels c and f). It also leads to increases over much of the North Atlantic with the exception of select regions over the center of the basin. In general, the increases in variance are most pronounced at high latitudes.

The increases in Northern Hemisphere temperature variability are more pronounced on on multiannual timescales. Figure 2 shows the fractional changes in surface temperature variability between the locked and interactive simulations for temperatures that have been one and three-year low pass filtered. Note that the colorscales are again different in the left and right columns. In general, cloud-circulation coupling plays an increasingly large role in surface temperature variability at increasingly long timescales. Importantly, cloud-circulation coupling leads to increases in extratropical multiannual variability of ~25-45% over most of the Northern Hemisphere oceans.

The increases in Northern Hemisphere temperature variability due to cloud-circulation coupling are also readily apparent in temperature data averaged over large spatial regions. For example, the center panel in Fig. 3 reproduces the fractional changes in three-year low-pass temperature variability from Fig. 2, and the surrounding panels show the changes in the standard deviations for temperatures that have been low-pass filtered and averaged over large spatial regions. The low-pass filter length is given on the abscissa of each panel, and the regions are defined in the caption. For example: Results at two years on the North Pacific panel indicate the fractional changes in temperature variability for output that have been 1) spatially-averaged over the North Pacific and then 2) two-year low-pass filtered. Cloud-circulation coupling leads to increases in area-mean temperature variance over all Northern Hemisphere regions and for all low-pass filters. The increases are ~10% over many land areas, approach ~25% over the North Atlantic, and reach nearly ~45% over the North Pacific sector.

Together, the results in Figures 1-3 indicate that cloud-circulation coupling contributes to surface temperature variability over much of the Northern Hemisphere. That the increases extend to low-frequency timescales has potentially important implications for the interpretation of decadal climate variability. The changes in persistence are not only apparent in the changes in the standard deviations (Figures 1-3), but also in time series of temperature averaged over key regions. For example, Figure 4 shows the time series of simulated temperature variability over the North Pacific and North Atlantic ocean basins. As is visually apparent from the time series, the interactive simulation (blue lines) has more variability on decadal timescales than the locked simulation (orange lines). For example, SSTs in the interactive simulation (blue) exhibit multiple examples of large shifts on decadal timescales tht are not apparent in the locked (orange) simulation.

Why does cloud/circulation coupling lead to increased variability in Northern Hemisphere surface temperatures? Following Yu and Boer (2006) and Li et al. (2020), the mechanisms that contribute to the temperature variance can be quantified from the surface energy budget. Starting with the thermodynamic energy equation at the surface:

$$C\frac{dT}{dt} = Q_{SW} + Q_{LW} + Q_{SH} + Q_{LH} \quad (1)$$

where $C$ is the effective heat capacity of the ocean mixed layer or land surface, $T$ is the surface temperature, and the $Q$ terms denote the fluxes of shortwave radiation, longwave radiation, latent heat, and sensible heat, respectively. The conversion of Eq. 1 into a diagnostic equation for the temperature variance involves 1) assuming all parameters in Eq. 1 reflect departures from the long-term mean; 2) replacing the derivative on the LHS with a centered differencing scheme; 3) squaring the resulting equation and taking the time average (see Li et al. (2020) for details of the procedure). The resulting expression for the temperature variance can be expressed as

$$\sigma_T^2 = G\sigma_\Sigma^2 e \quad (2)$$

where $\sigma_T^2$ denotes the surface temperature variance; $\sigma_\Sigma^2$ is the sum of the individual surface flux variances; $G = \frac{2(\Delta t)^2}{C^2(1-r_2)}$ is a 'transfer term' that accounts for the influence of persistence (as measured by the lag-two month autocorrelation $r_2$), the effective heat capacity ($C$), and the sampling time scale $\Delta t$ on temperature variance; and $e = 1 + \frac{2\Sigma\overline{Q_i Q_j}}{\sigma_\Sigma^2}$ is an 'efficiency term' that accounts for the covariances between the various surface fluxes (i.e., negative correlations between different fluxes lead to $e < 1$).

The ratios of the three terms in Eq. 2 calculated for the interactive and locked simulations are shown in Supporting Information Figure S1. As is the case in the tropics (Li et al., 2020), the increases in surface temperature variance in the extratropics between the interactive and locked runs are dominated by increases in the variances of the fluxes (i.e., increases in the $\sigma_\Sigma^2$ term). The efficiency term acts to reduce the effectiveness of the increases in the flux variances due to cross-correlations between the individual fluxes. The transfer term acts to modestly enhance the effectiveness of the increases in the flux variances over the oceans since the autocorrelation of the surface temperature field increases in the interactive simulation.

Figure 5 explores the changes in the variances of the various individual fluxes between the locked and interactive simulations. The first column shows the climatological-mean surface flux variances in the interactive simulation. In general, the latent, sensible, and shortwave radiative fluxes are most important for the total variance. The latent heat fluxes are dominant over the subtropical oceans, and the sensible heat fluxes have largest amplitudes over the western boundary current regions and along the periphery of the Arctic. The radiative flux variances are more spatially amorphous. The second column shows the attendant climatological-mean surface flux variances in the locked simulation, and the third column shows the fractional changes in the variance between the two simulations. By far the primary effect of cloud-circulation coupling is to enhance the variance of the shortwave and longwave radiative fluxes (panels c, g). The increases in the shortwave radiative flux variances are prominent across the hemisphere. The increases in the longwave radiative flux variances are relatively weak over ocean regions but comparable to the changes in the shortwave fluxes over terrestrial regions.

The increases in the variances of the shortwave radiative fluxes due to cloud-circulation coupling are consistent with the reddening of cloud fraction by the atmospheric flow (Li et al., 2020). The mechanism works as follows. In the presence of cloud-circulation coupling, cloud

fraction exhibits power spectra consistent with red noise since the cloud-fields are coupled to large-scale variability in the atmospheric circulation. When the cloud-fields are scrambled and thus decoupled from the circulation, the total variances of cloud fraction are preserved, but the variance is distributed roughly equally across all timescales since there is no persistence in the scrambled cloud-fields. As such, when clouds are coupled to the circulation, cloud fraction and shortwave CRE exhibit *less* variance on very short timescales (e.g., timescales of a few hours) but *more* variance on low frequency timescales (e.g., timescales longer than a few days). The above argument holds for the changes in the shortwave radiative flux variance shown in Fig. 5c, since the variance of the total shortwave flux is dominated by the variance of shortwave CRE. The argument holds for the component of the longwave radiative flux variance that reflects changes in longwave CRE, but it is likely that the changes in the longwave radiative flux variance shown in Fig. 5g also arise from changes in temperature variance.

## 4 Implications

Together, the results shown here indicate that cloud-circulation coupling has a pronounced effect on surface temperature variability in an Earth System Model across vast regions of the Northern Hemisphere. The results suggest that CRE play a key role in climate variability not only in the tropics (Rädel et al., 2016; Middlemas et al., 2019; Li et al., 2020), but also in the Northern Hemisphere. Importantly, prominent increases in variance are found over the North Pacific and North Atlantic basins, where cloud-circulation coupling increases the variance of multiannual to decadal SST variability by ~45% and ~25%, respectively. We have argued that the increases in extratropical SST variance arise from the same mechanism that contributes to the increases in tropical SST variance found in our previous study (Li et al. 2020): That is, cloud-circulation coupling acts to "redden" the variance of clouds and their shortwave radiative effects, and thus enhancing the contribution of CRE to low-frequency climate variability.

The results have important implications for the interpretation of observed climate variability. The variances of the surface fluxes in the interactive simulation bear very close resemblance to the observed fluxes, as estimated by ERA 5 (Hersbach et al., 2020, compare left and right columns in Fig. 5). Thus in the real-world, cloud-circulation coupling may be viewed as enhancing the variance of low-frequency temperature variability by roughly the same amount as that found in the differences between the interactive and locked simulations. In other words, the simulations shown here should provide a close approximation of the importance of cloud-circulation coupling for low-frequency temperature variability in Earth's climate.

Previous work has suggested that CREs have a relatively weak effect on extratropical climate variability (i.e., Papavasileiou et al. 2020; Li et al. 2020). However, the results shown here make clear that cloud-circulation coupling has a pronounced effect on Northern Hemisphere surface temperature variability, with the large increases in variance found over the extratropical oceans. Taken at face value, the results suggest that cloud-circulation coupling makes important contributions to multiannual to decadal variability in the Pacific Decadal Oscillation and Atlantic Multidecadal Variability.

## Acknowledgments

We thank Dirk Olonscheck for providing the model output used in this and the companion study Li, Thompson, and Olonscheck. We also thank Ying Li for analyses that provided the inspiration for exploring results on low-frequency timescales. CB and DWJT are supported by the NSF Climate and Large-Scale Dynamics Program.

## Open Research

Data Availability Statement:

All data for Figure 1-5 and Supplementary Figure S1 can be found at:

http://dx.doi.org/10.25675/10217/234116

## Figures

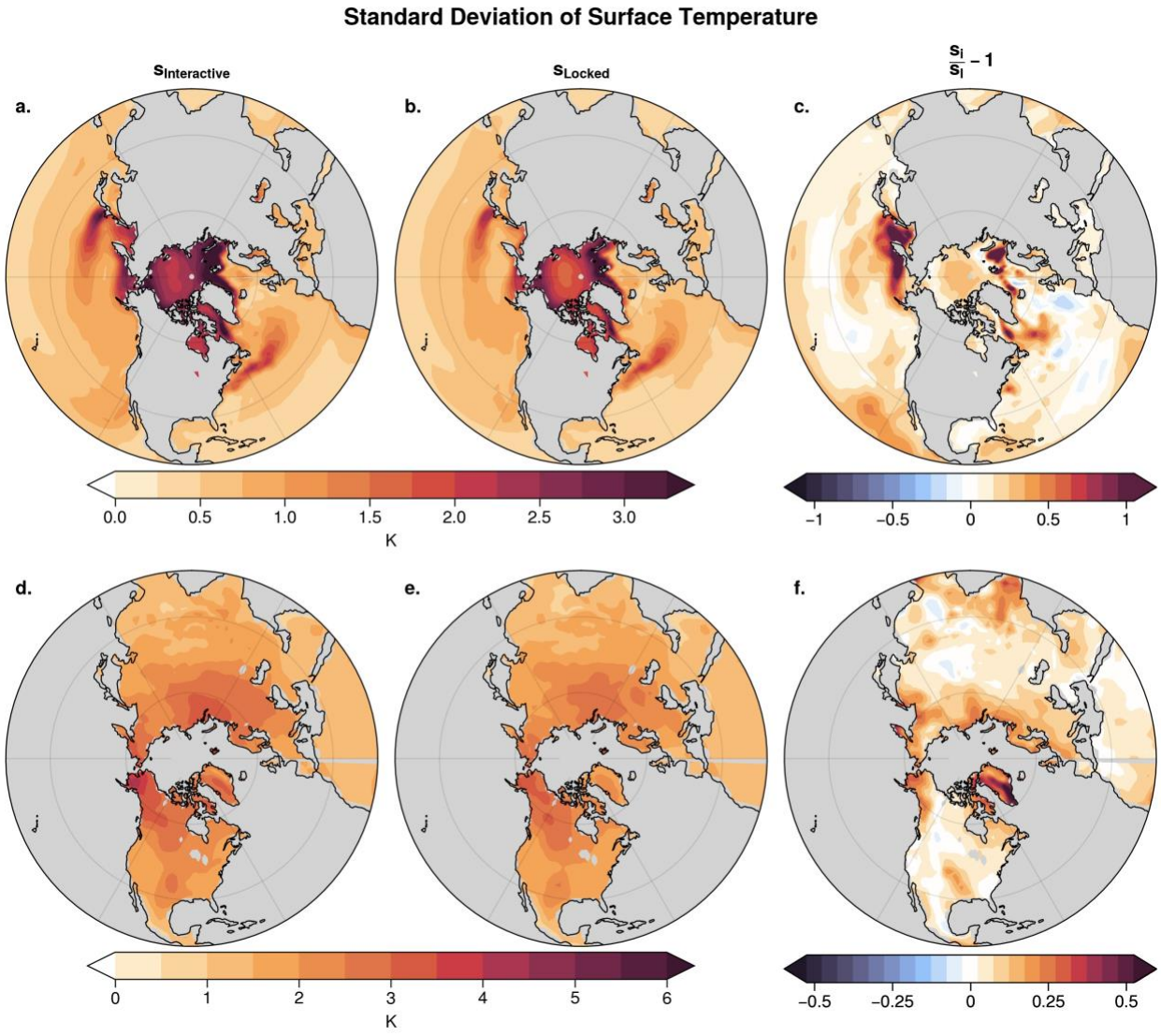


**Figure 1**. Monthly-mean surface temperature standard deviation across the Northern Hemisphere for (a,d) the 200-year interactive simulation and (b,e) the 200-year locked simulation. (c,f) The fractional changes in the standard deviations between simulations.

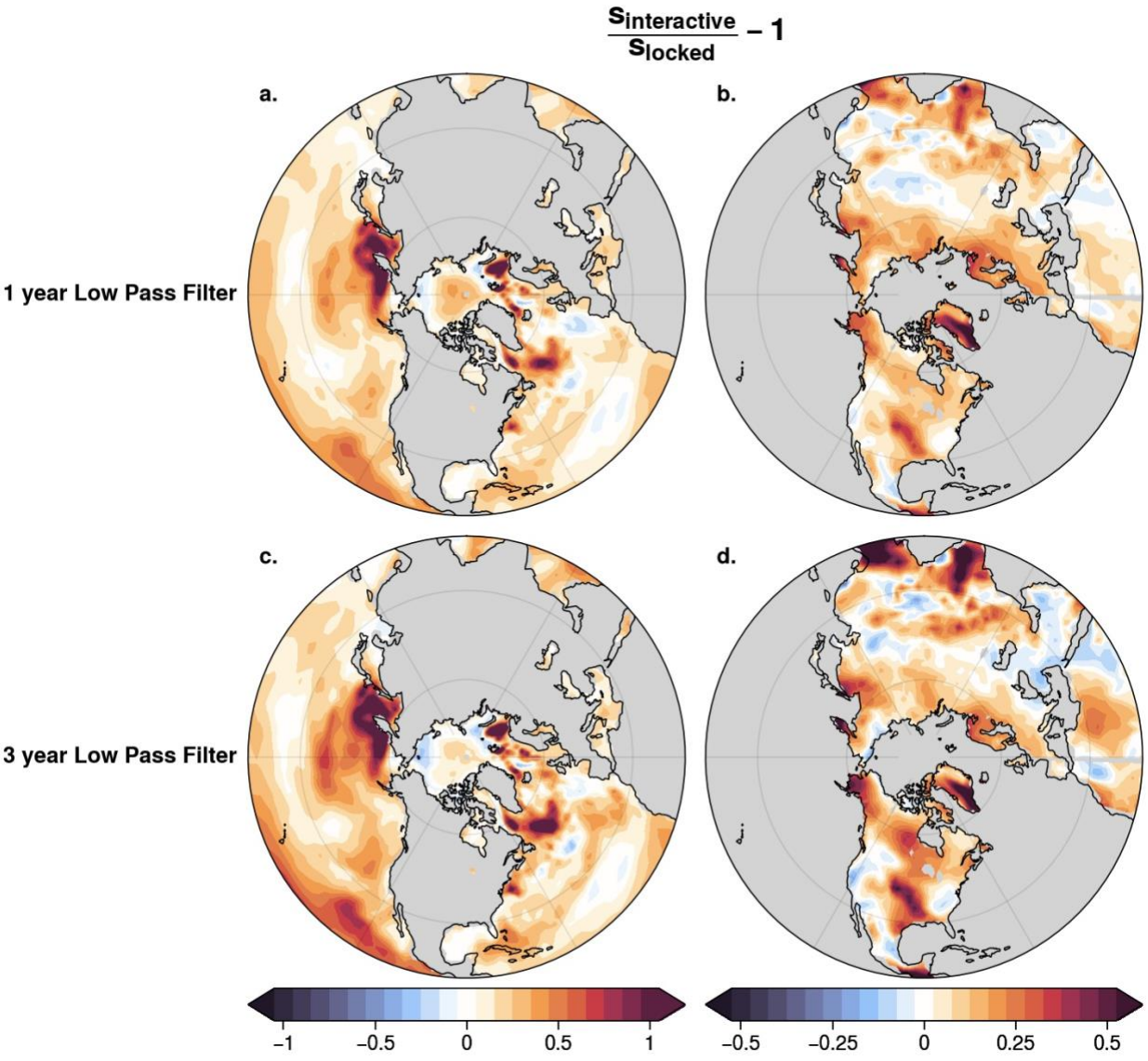


**Figure 2**. The fractional changes in surface temperature standard deviation between the locked-cloud and interactive simulations. (a,b) Temperatures have been one-year low-pass filtered. (c,d) Temperatures have been three-year low-pass filtered.

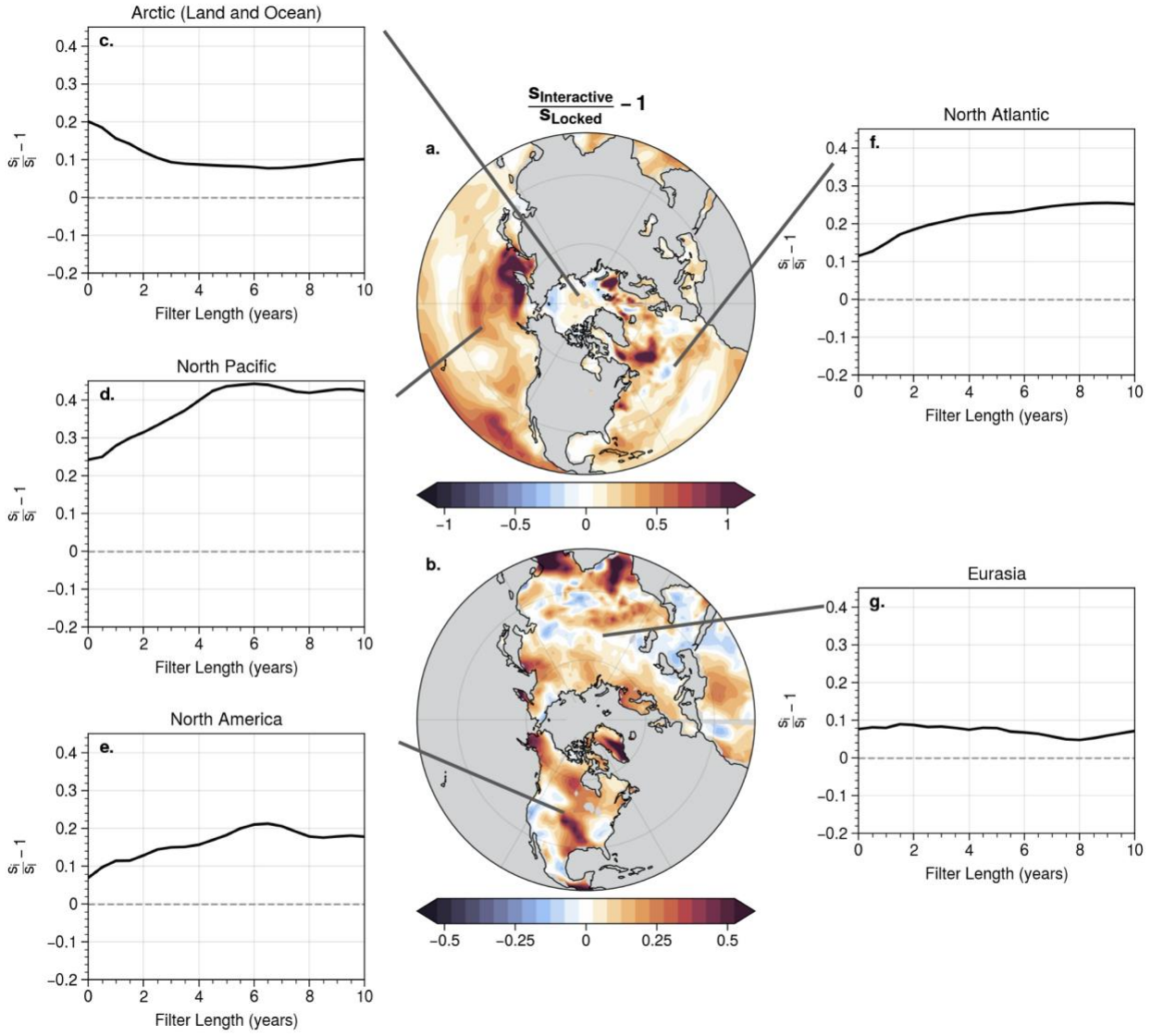


**Figure 3**. Changes in surface temperature variability for five different regions due to cloud-circulation coupling. (a,b) Fractional changes in three-year low-pass temperature variability reproduced from Fig. 2. Fractional changes in standard deviation of surface temperature for different low-pass filter lengths and averaged over (c) entire Arctic (60°-90°N), (d) North Pacific (15°-60°N, 129°E-241°E), (e) North America (15°-60°N, 196°-305°E), (f) North Atlantic (15°-60°N, 285°-360°E), (g) Eurasia (15°-60°N, 0°-170°E).

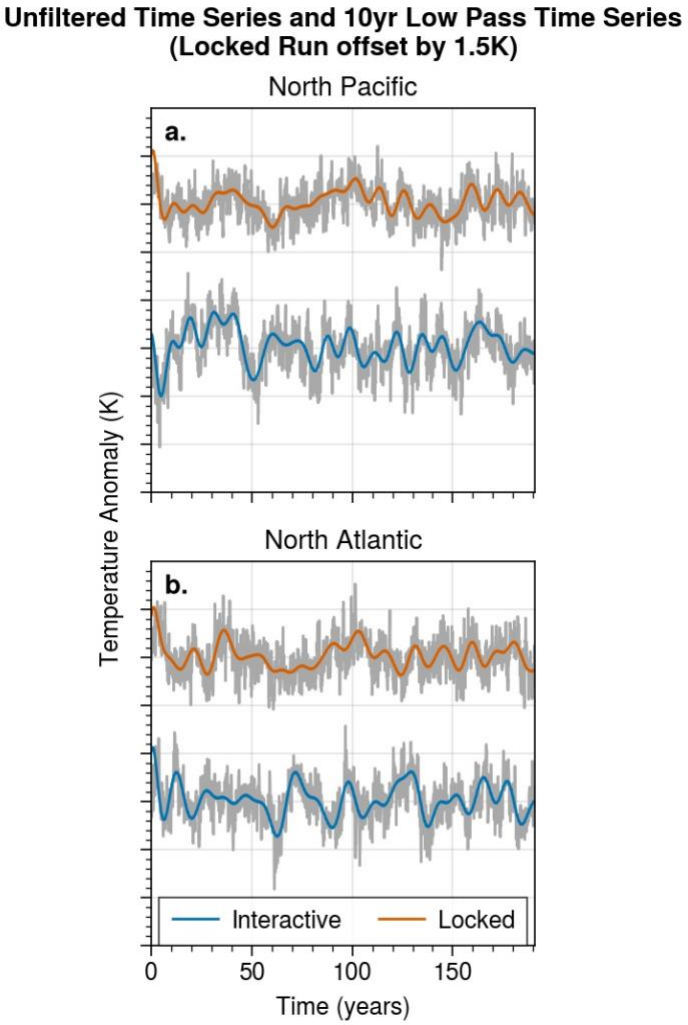


256

257 **Figure 4**. Area averaged monthly-mean time series of surface temperature anomalies for the
258 interactive and locked-cloud simulations over the (a) North Pacific and (b) North Atlantic
259 regions. Grayed lines show unfiltered time series, blue and orange lines indicate ten-year low
260 pass filtered time series for the interactive and locked-cloud simulations respectively. The time
261 series for the locked-cloud simulation is offset by 1.5K to distinguish the two time series.
262

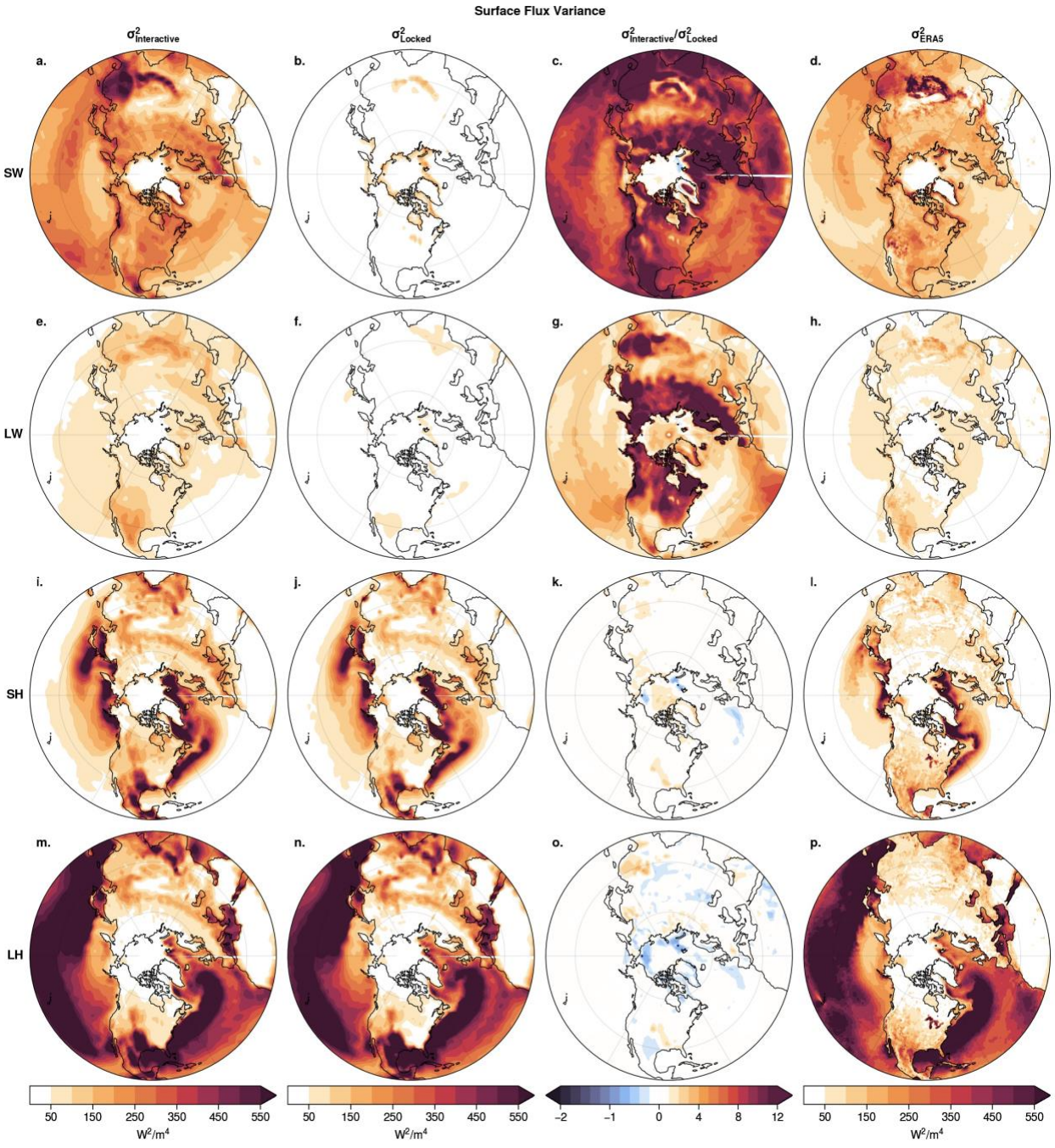


**Figure 5**. Surface energy flux variances: (a-d) surface shortwave radiative flux, (e-h) surface longwave radiative flux, (i-l) surface sensible heat flux, (m-p) surface latent heat flux. The first and second column show the individual flux variance for the interactive and locked-cloud simulations respectively. The third column shows the ratio of individual surface flux variance between the interactive and locked-cloud simulation. The fourth column shows the surface flux variances as estimated by ERA 5 reanalysis.

## References


Albern, N., Voigt, A., Buehler, S. A., & Grützun, V. (2018). Robust and Nonrobust Impacts of Atmospheric Cloud-Radiative Interactions on the Tropical Circulation and Its Response to Surface Warming. *Geophysical Research Letters*, *45*(16), 8577–8585. https://doi.org/10.1029/2018GL079599

Albern, N., Voigt, A., & Pinto, J. G. (2019). Cloud-Radiative Impact on the Regional Responses of the Midlatitude Jet Streams and Storm Tracks to Global Warming. *Journal of Advances in Modeling Earth Systems*, *11*(7), 1940–1958. https://doi.org/10.1029/2018MS001592

Albern, N., Voigt, A., Thompson, D. W. J., & Pinto, J. G. (2020). The Role of Tropical, Midlatitude, and Polar Cloud-Radiative Changes for the Midlatitude Circulation Response to Global Warming. *Journal of Climate*, *33*(18), 7927–7943. https://doi.org/10.1175/JCLI-D-20-0073.1

Boehm, C., & Thompson, D. W. J. (2021). Data Associated with "The Contribution of Clouds to Northern Hemisphere Surface Temperature Variability on Monthly to Decadal Timescales" [Dataset]. Colorado State University. Libraries. http://dx.doi.org/10.25675/10217/234116

Bony, S., & Dufresne, J.-L. (2005). Marine boundary layer clouds at the heart of tropical cloud feedback uncertainties in climate models. *Geophysical Research Letters*, *32*(20). https://doi.org/10.1029/2005GL023851

Bony, S., Stevens, B., Frierson, D. M. W., Jakob, C., Kageyama, M., Pincus, R., Shepherd, T. G., Sherwood, S. C., Siebesma, A. P., Sobel, A. H., Watanabe, M., & Webb, M. J. (2015). Clouds, circulation and climate sensitivity. *Nature Geoscience*, *8*(4), 261–268. https://doi.org/10.1038/ngeo2398

Ceppi, P., & Hartmann, D. L. (2016). Clouds and the Atmospheric Circulation Response to Warming. *Journal of Climate*, *29*(2), 783–799. https://doi.org/10.1175/JCLI-D-15-0394.1

Grise, K. M., Medeiros, B., Benedict, J. J., & Olson, J. G. (2019). Investigating the Influence of Cloud Radiative Effects on the Extratropical Storm Tracks. *Geophysical Research Letters*, *46*(13), 7700–7707. https://doi.org/10.1029/2019GL083542

Hersbach, H., Bell, B., Berrisford, P., Hirahara, S., Horányi, A., Muñoz-Sabater, J., Nicolas, J., Peubey, C., Radu, R., Schepers, D., Simmons, A., Soci, C., Abdalla, S., Abellan, X., Balsamo, G., Bechtold, P., Biavati, G., Bidlot, J., Bonavita, M., … Thépaut, J.-N. (2020). The ERA5 global reanalysis. *Quarterly Journal of the Royal Meteorological Society*, *146*(730), 1999–2049. https://doi.org/10.1002/qj.3803

Li, Y., Thompson, D. W. J., & Olonscheck, D. (2020). A Basic Effect of Cloud Radiative Effects on Tropical Sea Surface Temperature Variability. *Journal of Climate*, *33*(10), 4333–4346. https://doi.org/10.1175/JCLI-D-19-0298.1

Middlemas, E. A., Clement, A. C., Medeiros, B., & Kirtman, B. (2019). Cloud Radiative Feedbacks and El Niño–Southern Oscillation. *Journal of Climate*, *32*(15), 4661–4680. https://doi.org/10.1175/JCLI-D-18-0842.1

Olonscheck, D., Mauritsen, T., & Notz, D. (2019). Arctic sea-ice variability is primarily driven by atmospheric temperature fluctuations. *Nature Geoscience*, *12*(6), 430–434. https://doi.org/10.1038/s41561-019-0363-1

Papavasileiou, G., Voigt, A., & Knippertz, P. (2020). The role of observed cloud-radiative anomalies for the dynamics of the North Atlantic Oscillation on synoptic time-scales. *Quarterly Journal of the Royal Meteorological Society*, *146*(729), 1822–1841. https://doi.org/10.1002/qj.3768

Rädel, G., Mauritsen, T., Stevens, B., Dommenget, D., Matei, D., Bellomo, K., & Clement, A. (2016). Amplification of El Niño by cloud longwave coupling to atmospheric circulation. *Nature Geoscience*, *9*(2), 106–110. https://doi.org/10.1038/ngeo2630

Schäfer, S. A. K., & Voigt, A. (2018). Radiation Weakens Idealized Midlatitude Cyclones. *Geophysical Research Letters*, *45*(6), 2833–2841. https://doi.org/10.1002/2017GL076726

Sherwood, S. C., Webb, M. J., Annan, J. D., Armour, K. C., Forster, P. M., Hargreaves, J. C., Hegerl, G., Klein, S. A., Marvel, K. D., Rohling, E. J., Watanabe, M., Andrews, T., Braconnot, P., Bretherton, C. S., Foster, G. L., Hausfather, Z., von der Heydt, A. S., Knutti, R., Mauritsen, T., … Zelinka, M. D. (2020). An Assessment of Earth's Climate Sensitivity Using Multiple Lines of Evidence. *Reviews of Geophysics*, *58*(4), e2019RG000678. https://doi.org/10.1029/2019RG000678

Stephens, G. L., Li, J., Wild, M., Clayson, C. A., Loeb, N., Kato, S., L'Ecuyer, T., Stackhouse, P. W., Lebsock, M., & Andrews, T. (2012). An update on Earth's energy balance in light of the latest global observations. *Nature Geoscience*, *5*(10), 691–696. https://doi.org/10.1038/ngeo1580

Voigt, A., & Albern, N. (2019). No Cookie for Climate Change. *Geophysical Research Letters*, *46*(24), 14751–14761. https://doi.org/10.1029/2019GL084987

Voigt, A., Albern, N., Ceppi, P., Grise, K., Li, Y., & Medeiros, B. (2021). Clouds, radiation, and atmospheric circulation in the present-day climate and under climate change. *WIREs Climate Change*, *12*(2), e694. https://doi.org/10.1002/wcc.694

Voigt, A., & Shaw, T. A. (2015). Circulation response to warming shaped by radiative changes of clouds and water vapour. *Nature Geoscience*, *8*(2), 102–106. https://doi.org/10.1038/ngeo2345

Voigt, A., & Shaw, T. A. (2016). Impact of Regional Atmospheric Cloud Radiative Changes on Shifts of the Extratropical Jet Stream in Response to Global Warming. *Journal of Climate*, *29*(23), 8399–8421. https://doi.org/10.1175/JCLI-D-16-0140.1

Yu, B., & Boer, G. J. (2006). The variance of sea surface temperature and projected changes with global warming. *Climate Dynamics*, *26*(7), 801–821. https://doi.org/10.1007/s00382-006-0117-9

Zelinka, M. D., & Hartmann, D. L. (2010). Why is longwave cloud feedback positive? *Journal of Geophysical Research: Atmospheres*, *115*(D16). https://doi.org/10.1029/2010JD013817

*Geophysical Research Letters*

Supporting Information for

# The Contribution of Clouds to Northern Hemisphere Surface Temperature Variability on Monthly to Decadal Timescales

Chloe Boehm[1], David W.J. Thompson[1,2]

[1]Department of Atmospheric Science, Colorado State University, Fort Collins, CO, USA

[2]School of Environmental Sciences, University of East Anglia, Norwich, UK

## Contents of this file



## Introduction

The ratios of the three terms in Eq. 2 calculated for the interactive and locked simulations are shown in this supporting information.

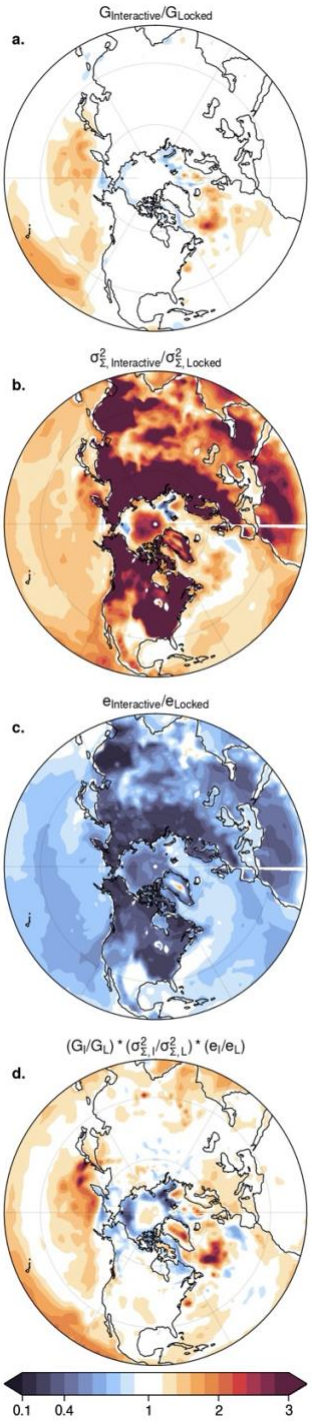


**Figure S1.** The ratio for each term of the diagnostic equation for surface temperature variance (Eq. 2) between the interactive and locked simulation. (a-c) Calculated ratios for the three terms on the right-hand side of Eq. 2 between the interactive and locked simulations. (d) Recreated surface temperature variance ratio between interactive and locked simulations by multiplying each term in Eq. 2.